Results in Engineering 22 (2024) 102009

Contents lists available at ScienceDirect

Results in Engineering

journal homepage: www.sciencedirect.com/journal/results-in-engineering

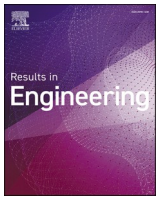

Slip strength of COR-TEN and Zn-coated steel preloaded bolted joints

L. Collini *, R. Garziera, A. Corvi, G. Cantarelli

Department of Engineering and Architecture – University of Parma, Viale Delle Scienze 181/A, 43124, Parma, Italy

ARTICLE INFO

Keywords:
Slip factor
Preloaded bolted joint
COR-TEN steel
Zn-coated steel

ABSTRACT

Knowledge of the effective slip strength is a crucial safety issue when a bolted connection is designed to work by friction. Even if technical standards indicate the necessary tightening torque to obtain the desired preload, experimental relationship between bolt torque and preload is required in many cases where surface and bolt conditions are uncertain. In this work, the torque–preload relationship and the effective slip factors of bolted joints operating under non-standard surface conditions, namely COR-TEN and Zn-coated plates, are determined experimentally, and compared with standard as-rolled data. Results indicate that the requirements of design standards are not always conservative, making experimental characterization of the joint necessary.

1. Introduction

1.1. Brief historical overview

In a pioneering work by Whittermore et al. in 1931, the relationship between applied torque and axial load was determined experimentally for a wide range of "thread locking devices" [1]. Since this comprehensive work was published, this mechanical fastening system has essentially undergone no further developments.

In the years that followed, many studies were published relating to specific conditions or situations in which thread-locking devices were to operate, with particular attention paid to friction phenomena. Improvements in technology and metal working processes after about 90 years, together with more refined measurement methods, made it possible to better understand the mechanical quantities such as forces involved in the process of tightening a bolt. For example, Jiang et al. precisely measured the thread friction and the bearing friction between the nut and clamped surfaces, performing statistical analysis to allow reliability assessment of the bolted joints in terms of clamping force control [2]. Nassar et al. investigated the effect of surface roughness on the torque-tension relationship in threaded fasteners. Different levels of surface roughness were considered for the fastener/washer and joint surfaces, with torque-tension data expressed in terms of the nut factor [3,4]. Bickford proposed a procedure for studying friction in standard fasteners based on the experimentally determined effective bearing friction radius, underhead friction coefficient, and thread friction [5]; again, in Ref. [6] Croccolo et al. define an experimental methodology to determine the friction coefficients in bolted joints thus relating the tightening torque to the preload; recently, Hinse et al. precisely determined the friction coefficients in a bolt-nut connection by optical measurement [7]; Shi et al. analysed the shear behavior of high-strength bolts connection with the aim of adopting a simplified spring model for engineering applications based on FEA [8]; similar work is proposed by Wang et al. where bolts work in traction on a flush end-plate connection [9].

Following on from the work of Whittermore et al., in 1931, subsequent works therefore brought greater accuracy in determining the value of torque components required to overcome friction in threaded fasteners, yielding more reliable torque-tension correlations to enhance the safety and quality of bolted assemblies.

1.2. Current design methods and recommendations

The schematic in Fig. 1 shows the torque distribution in a tightened bolted joint. The tightening torque is mostly consumed in overcoming the combined effect of two frictional torque components. The first is nut/washer friction during tightening, assuming the head is still; the second is thread friction. After overcoming friction, the remaining torque component, comprising about 10% of the total, produces the fastener tension and creates the joint clamping force, [2,10].

The torque-tension relationship in threaded fasteners is highly sensitive to variations in friction torque.

Moderate variations, which are common in industrial applications, can have significant impact on the stability of the clamp load in bolted assemblies [8,11,12]. Recent studies have highlighted the fact that

* Corresponding author.
E-mail addresses: luca.collini@unipr.it (L. Collini), rinaldo.garziera@unipr.it (R. Garziera), alberto.corvi@unipr.it (A. Corvi), giancarlo.cantarelli@unipr.it (G. Cantarelli).

https://doi.org/10.1016/j.rineng.2024.102009
Received 20 October 2023; Received in revised form 5 March 2024; Accepted 8 March 2024
Available online 16 March 2024

Nomenclature

$M_{p,i}$	bolt tightening torque
F_b	bolt load
$F_{p,C}$	specified preload, equal to $0.7f_{ub}A_s$
$F_{S,i}$	individual slip load
F_{Sm}, s_{Fs}	slip load mean value and standard deviation
$F_{s,Rd}$	design slip resistance per bolt at ultimate limit state
A_s	bolt net cross-section
f_{ub}	bolt ultimate tensile strength
d	nominal bolt diameter
p	thread pitch
μ_t	friction coefficient of threads
μ_c	friction coefficient of collar
μ_i	individual slip factor
μ_m, s_μ	slip factor mean value and standard deviation
r_i	thread average radius
r_c	washer average radius
R_q	root mean square roughness
lr	roughness sampling length
α	thread angle
k_i	bolt performance factor
μ_k	dynamic surface friction coefficient
μ_s	static surface friction coefficient
d_c	decay coefficient
γ_{eq}	slip displacement
γ_{M3}	partial safety factor at ultimate limit state
k_s	bolt hole factor
F_C	Coulomb friction force
F_V	viscous friction force
F_S	static friction force
v, v_s	slip velocity, Stribeck characteristic velocity

friction stresses only appear near bolt holes, with stress on the contact surface exhibiting a ring distribution around the hole [13]. The stress is largest at the edge of the bolt hole, decreased to nearly zero at a certain distance from the edge. The friction stress distribution on the contact surface can be represented as a contact stress over a near-circular region called the *pressure effect region*.

Problems pertaining to structural dynamics with bolted joints have also been addressed in various studies, such as [14]. These problems are complex in nature because each joint is affected by different sources of uncertainty and non-smooth, non-linear characteristics. For example, contact forces are never perfectly planar due to manufacturing tolerances during production of contact surfaces, while initial forces are non-uniformly distributed in the presence of lateral loads. This is in addition to the prying load, which leads to non-linear tension in the bolt and non-linear compression in the joint. Under dynamic and vibrational environmental loading, the joint preload experiences some relaxation that results in time variation of the structure's dynamic properties. Most of the reported studies focus on the energy dissipation of bolted joints, linear and non-linear identification of the dynamic properties of joints, parameter uncertainties and relaxation, and active control of joint preload.

In relation to international specifications and guidelines, European [15–17], American [18,19] and British [20] codes and standards have been refined to regulate sizing calculations for the safe design of connections and bolted joints. Different approaches are followed in considering the slip strength of bolted connections, depending on the friction coefficients, calculation model, and failure mechanisms of the *bolt system*. In the present work, experimental results will be compared with predictions from these models. In Europe, two technical solutions exist to achieve the necessary ductility of bolt/nut/washer assemblies for preloaded structural bolts (HR and HV systems) [21]. It is therefore the responsibility of experts using structural bolts to use one system or the other. However, preloaded bolted assemblies are very sensitive to differences in manufacturing and lubrication that can directly determine friction conditions. Furthermore, increased safety and material performance requirements, including bolt resilience and strength, mean that friction coefficients used in calculations are of primary importance. Guidelines currently rely on a statistical approach to determine the relationship between applied preload torque and developed bolt force within a standard bolt/nut/washer assembly, in which the bolt/washer contact is known and can be controlled.

On the other hand, much less is known about the effective friction conditions at joint surfaces due to the large variability of surface finishing and operating conditions. Despite numerous studies aimed at determining the slip resistance of bolted assemblies, new materials and evolving surface treatments make it necessary to continuous test systems to guarantee high safety standards.

For example, the use of COR-TEN structural steel in large constructions such as bridges and buildings is relatively new, with the effective friction being uncertain or in some cases unknown. Other factors such as environmental dust, lubricants, vibration, or repeated tightening, are difficult to predict and are taken into consideration only by increasing the safety factor and, consequently, decreasing the efficiency of the structural bolting design.

In this work, knowledge of slip resistance and analysis of friction phenomena are extended to non-standard conditions comprising S235J2WP COR-TEN, Zinc-coated, and standard As Rolled (AR) S235J steel, arbitrary chosen to represent a certain variety of applications. Slip

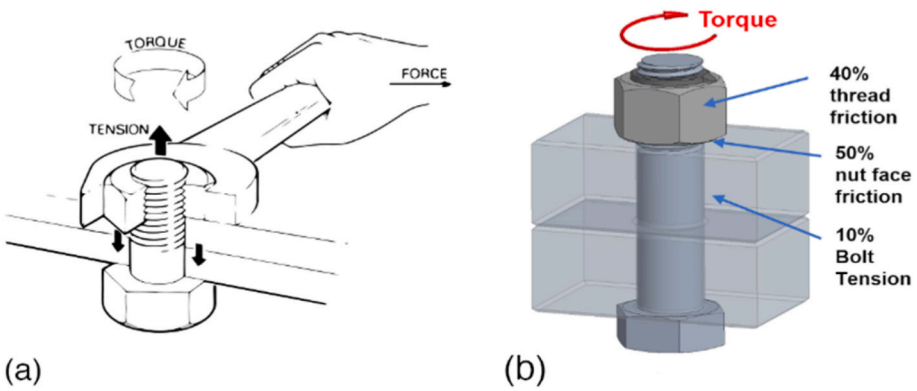

Fig. 1. Schematic of torque distribution in a tightened bolt.

resistance is obtained through laboratory testing of special joints, with considerations relating to data dispersion drawn based on the measured surface topography. A FEA model is also developed to analyse slip dynamics. The most relevant conclusion is that, depending on the surface conditions, the requirements of design standards are not always conservative, with experimental characterisation of the joint required.

2. Experimental setup and procedure

2.1. Specimens and experimental setup

Slip factors were determined experimentally using double butt-strap joints in line with EN-1090 [22], reported in Fig. 2. As required by this standard, the two inner plates have been produced at the CNC machines by cutting them consecutively from the same piece of material and assembling them in their original relative positions to obtain the same thickness, with edges and surfaces accurately cut so as not to interfere with contact between the plate surfaces. Two different inner plate thicknesses have been then tested, 16 mm and 20 mm, clamped with 8.8 class M16 and M20 bolts, respectively. Three different plate surface conditions were investigated, shown in Fig. 3(a). The dimensions of the specimens are summarized in Table 1.

The employed specimen geometry permitted two slip plane couples to be activated separately during tensile loading, 1–2 and 3–4 in Fig. 2, yielding two average values of friction coefficient for each test, as specified in section 2.2.

Slip could occur in failure modes comprising a combination of slip in planes 1 and 2 or 3 and 4, or diagonally in slip planes 1 and 4 or 2 and 3. The test was carried out on an MTS 810 universal material testing system by loading the specimen with a load-controlled ramp at a constant load rate of 9 kN/min while recording the load–slip curve and, in the case of M16 specimens, the exerted bolt axial load via a calibrated annular load cell. The set-up is illustrated in Fig. 3(b) and (c). According to Ref. [22], the slip strength is evaluated as the peak force signal or the load at 0.15 mm slip, deducted from the force–displacement recorded diagram. A series of 8 test with at least 2 repetitions is performed for each of the considered finishes, in such a way as to get the minimum number of test required by the norm considering the standard deviation around the mean value.

All tested surface finishes are specified in Table 1. COR-TEN and Zn-coated specimens were compared with as-rolled S235J structural steel, with all plates being commercial varieties obtained by hot rolling. EN standard S235J2WP COR-TEN weathering steel plate was used for specimen S16-3 [24]. This is a very common hot rolled steel that is resistant to atmospheric corrosion, containing alloying elements such as chromium, nickel, and copper, as well as phosphorous, to achieve excellent corrosion protection qualities. As S235J2WP steel reacts with elements in the atmosphere, the material forms a layer of rust over time, which protects the underlying steel from further corrosion. The Zinc-coated finish was a commercial hot dip galvanised coating obtained by dipping the steel plates in a zinc melt. Profilometer analysis revealed a uniform coating about 100–120 μm thick, in line with ISO 1461:2022 [25].

2.2. Data processing

During each test, bolts were preloaded with $F_{p,C} = 0.7 f_{ub} A_s$ as required by ISO 1461, applying the tightening torque with a torque wrench. The preload was measured with an annular cell for all M16 specimens and compared with the classical relationship between applied torque $M_{p,i}$ and bolt axial load F_b, shown in Eq. (1):

$$M_{p,i} = \left(\frac{p}{2\pi} + \frac{\mu_t r_i}{\cos\alpha} + \mu_c r_c\right) F_b \tag{1}$$

where μ_t and μ_c are the friction coefficients between the screw and nut threads, and collar portion, respectively. The three terms in Eq. (1) represent the torque necessary to elongate the bolt, the part required to overcome friction in threads with an average radius of r_t and angle of α,

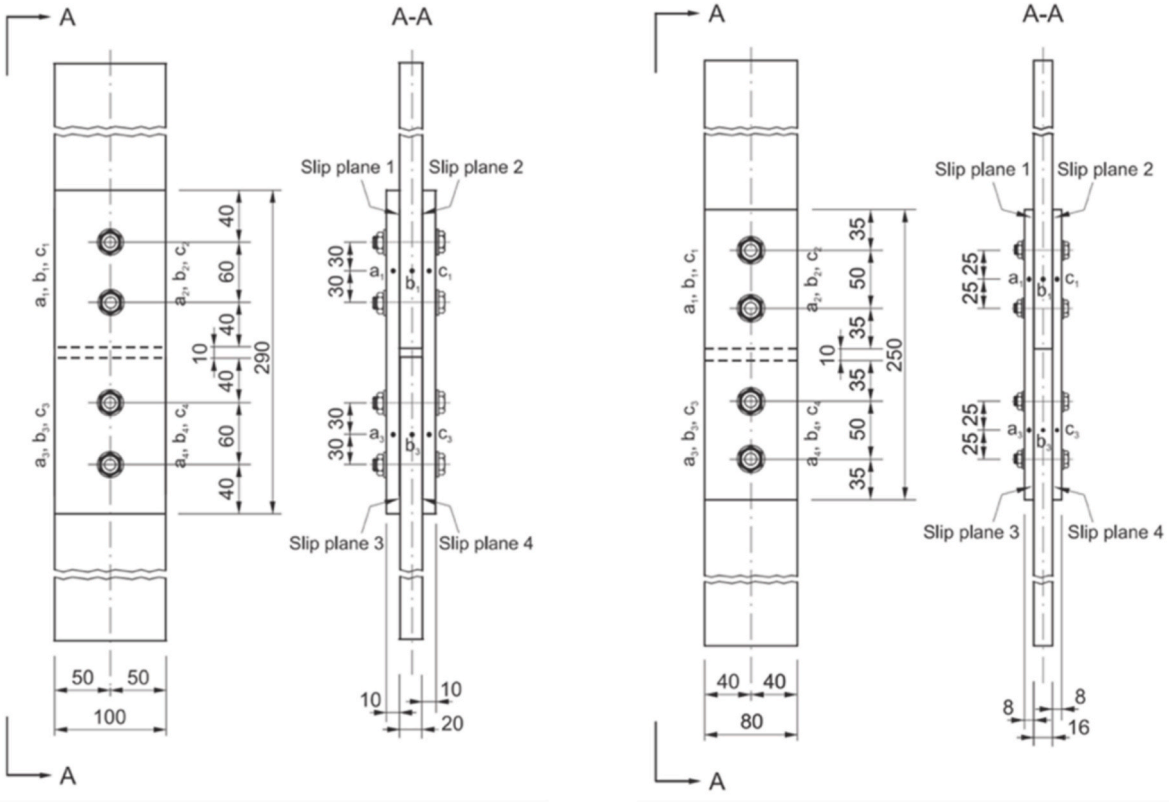

Fig. 2. Dimensions of specimens in EN-1090 [22].

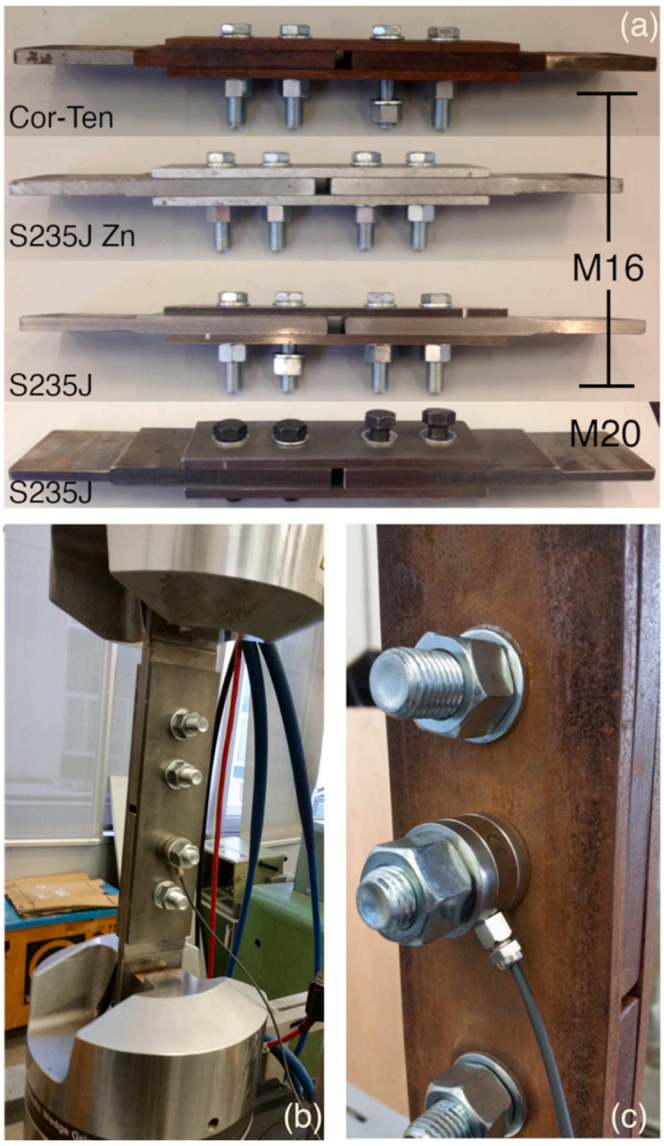

Fig. 3. (a) Specimens, (b) experimental setup, (c) load cell detail.

Table 1
Tested specimens and surface conditions.

Specimen	Plate thickness (mm)	Bolts	Surface condition
S16-1	8 + 16+8	4xM16 class 8.8	AR S235J steel [23]
S16-2	8 + 16+8		COR-TEN steel [24]
S16-3	8 + 16+8		Zinc-coated [25]
S20-1	10 + 20+10	4xM20 class 8.8	AR S235J steel

and the part required to overcome bolt/washer friction with an average radius of r_c. As discussed previously, the first term alone is responsible for system preloading. Recent standards express the bolt assembly efficiency in terms of a *k*-factor related to the *k*-classes k_1 and k_2:

$$k_i = \frac{M_{pi}}{dF_{p,C}} \tag{2}$$

where $F_{p,C}$ is the required preload, M_{pi} is the corresponding torque, and $k = 0.10–0.16$ and 0.10–0.23 for classes 1 and 2, respectively [21]. The following simplified relation is also still often employed:

$$M_{p,i} = 0.2F_b d \tag{3}$$

The individual slip factors were determined following prescription of [22] by Eq. (4):

$$\mu_i = \frac{F_{Si}}{4F_{p,C}}, \tag{4}$$

where F_{Si} is the individual slip load, and F_{Sm} and μ_m are the mean values of slip load and slip factor, together with their standard deviations:

$$F_{Sm} = \frac{\sum F_{Si}}{n}, s_{Fs} = \sqrt{\frac{\sum (F_{Si} - F_{Sm})^2}{n-1}} \tag{5}$$

$$\mu_m = \frac{\sum \mu_i}{n}, s_\mu = \sqrt{\frac{\sum (\mu_i - \mu_m)^2}{n-1}}$$

Two slips often occur per test, one per side of the joint, with the amount of slip depending on the initial position of the bolts before tightening and each bolt working in shear at the end of each slip. The final *characteristic* value of the slip factor is calculated as the 5 % fractile value with 75% confidence level [22].

2.3. Roughness measurements and FE modelling

Two complementary activities were conducted in parallel to the experimental to understand and model the observed slipping phenomenon. Surface topography was acquired in both unmodified and slipped regions with a Taylor Hobson CCI MP-L optical profiler to analyse friction mechanisms at the microscale. Based on the acquired topography profiles, the root mean squared roughness, R_q, was calculated in each case:

$$R_q = \sqrt{\frac{1}{l_r}\int_0^{l_r} Z^2(x)dx} \tag{6}$$

A FE analysis was also developed using Simulia ABAQUS© 2020 software to reproduce joint slipping and trying the fitting of experimental data. A standard Coulomb friction model was assumed for two of the three cases, with no relative motion taking place where the equivalent frictional stress, proportional to the contact pressure via the friction coefficient μ, was less than the critical stress. In this case, a kinetic, isotropic friction model was adopted for the plate contact for the AR and COR-TEN conditions:

$$\mu = \mu_k + (\mu_s - \mu_k)^{-d_c\dot{\gamma}_{eq}} \tag{7}$$

where μ_k is the kinetic friction coefficient, μ_s is the static friction coefficient, d_c is a user-defined decay coefficient, and $\dot{\gamma}_{eq}$ is the slip rate [26]. The model by Hess and Soom [27], instead, is used to reproduce the sliding dynamics of Zn-coated plates adding a viscous term, and implemented within the *FRIC subroutine available in ABAQUS© in the form:

$$F_f(v) = F_C + \frac{F_S - F_C}{1 + (v/v_s)^2} + F_v v \tag{8}$$

where the Coulomb, viscous and static friction components are denoted by F_C, F_v and F_s respectively, and v_s is the characteristic velocity of the Stribeck curve [28]. In all simulations, the other activating contact between the washers and plates was modelled as a penalty contact with friction coefficient μ varying from 0.18 to 0.2.

A symmetrical FE numerical model of the M16 specimen is shown on Fig. 4. The mesh in the 1/8 reduced model consisted of 8690 nodes, and 5908 linear hexahedral elements of type C3D8R with reduced integration and 576 linear wedge elements of type C3D6. The mesh was made finer where pressure and stresses were concentrated around the holes. Simulations were run with a dynamic explicit procedure at the nominal preload tightening torque, with the aim of quantifying the entity and extension of contact pressure and reproducing the sliding process.

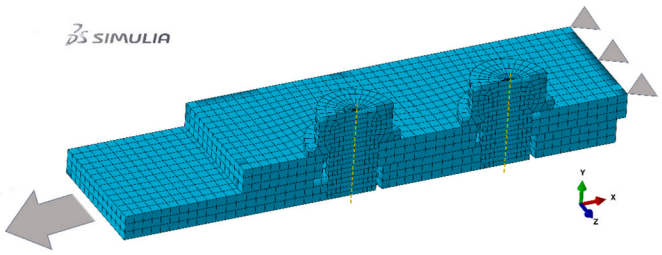

Fig. 4. FEA model of the M16 joint by Simulia ABAQUS©.

Proper definition of master/slave surfaces in the contact pair was important to facilitate the simulation, in which the penalty contact algorithm was chosen to allow element-based rigid surfaces to not be restricted to acting only as master surfaces. An elastic slip distance equal to 0.5 mm was also defined, with the automatic stabilization option activated to correctly manage stick-slip oscillations between the contact nodes.

Displacement boundary conditions were imposed at the extremities to impose the tensile load. The contact surfaces were modelled under the bolt heads and nuts, as well as between the plates, with the option of hard normal contact behaviour, assuming the same friction model for the two plate couples of each joint. The bolt preload was tuned over the same range as experiments (i.e. torque 50–350 Nm) using the *preload* function available in ABAQUS©. The calculus was repeated in a recursive manner tuning the coefficients in Eqs. (7) and (8) to match the experimental load-displacement curves within 2%.

3. Results and discussion

As no significative differences were observed between results obtained with M16 and M20 joints in the *as-rolled* condition, no distinction will be made between the two in the following sections, with results relating to M16 and M20 specimens merged into a single dataset.

3.1. Preload and slip behaviour

The load–displacement curves of the tested M20 joints and three families of M16 joints are shown in Fig. 5, with several curves presented with increasing bolt tightening torque. Typical slick-slip contact behaviour can be observed. As expected, the slip tensile load increases as bolt torque increases; however, different behaviour can be observed depending on the preload and, in particular, the surface finish. The slip load is clearly defined for AR and COR-TEN samples, while this is not the case for Zn-coated plates, which exhibit *creep* slipping. This is due to different friction mechanisms occurring between the Zn-coated surfaces. This phenomenon has been reported in the literature [29]. For AR and COR-TEN plates, a double peak can be observed followed by a plateau, regardless of the applied torque, in line with the classical process of friction increasing to a peak value and then decreasing before falling to a stable value.

Slip factors were calculated in line with EN 1090–2:2018 [22] using Eq. (4) for peak loads and Eq. (5) for mean values and dispersion. The calculated averaged slip factors and measured preloads are shown in Fig. 6(a) and (b), respectively, as functions of the applied torque applied to achieve the bolt preload.

As can be observed in Fig. 6(a), AR steel exhibits lower friction than COR-TEN and Zn-coated plates, with a slight decrease in all cases as torque increases. The slip strength of COR-TEN joints, however, appears to be less sensitive to the bolt load. Averaged slip factors are plotted together with data from the literature in Fig. 7. Reference slip factors found in literature for the same contact surface finish show a huge variability, ranging from 0.15 to 0.6.

The resulting average values and standard deviations of the present study were: $\mu_m = 0.242$ $s_\mu = 0.026$ for AR, $\mu_m = 0.372$ $s_\mu = 0.031$ for COR-TEN, and $\mu_m = 0.298$ $s_\mu = 0.030$ Zn-coated. These values are within the range of friction coefficients reported in the literature for similar

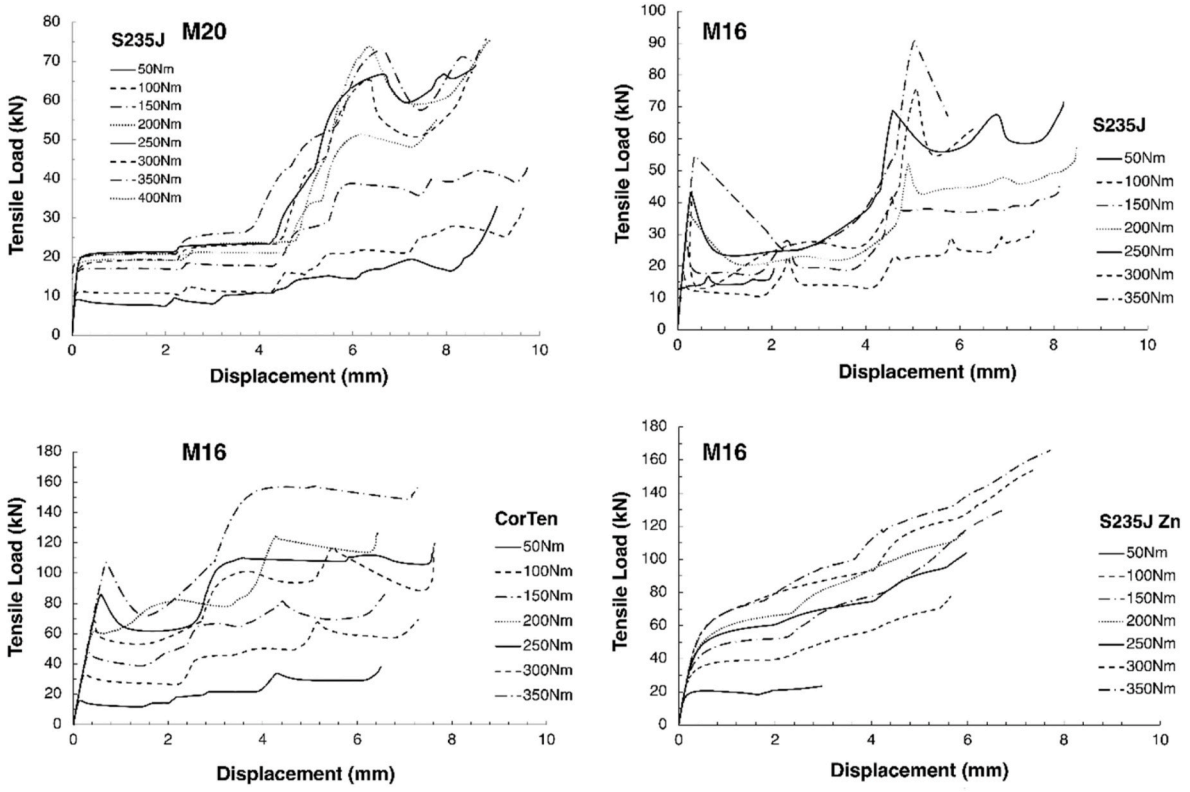

Fig. 5. Load–displacement curves (1st repetition) for (a) standard, (b) COR-TEN, (c) Zn-coated S235J steel joints.

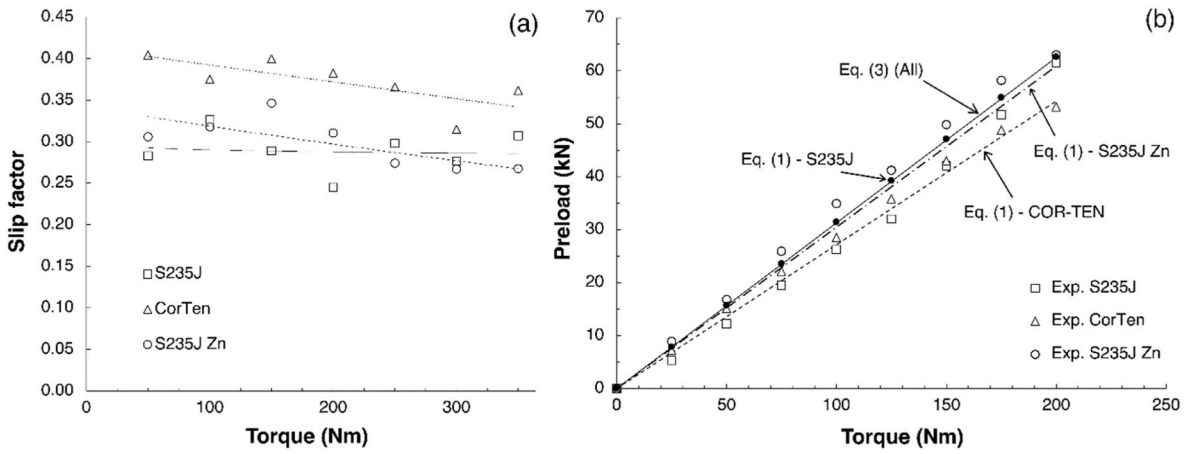

Fig. 6. (a) Slip factors and (b) Measured preloads.

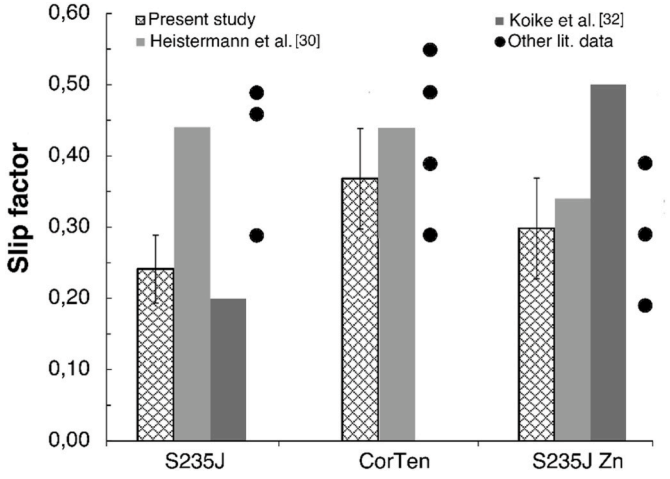

Fig. 7. Slip factors – mean and standard deviation – of the present investigation and reference data.

surfaces. Eccles et al., and Heistermann et al. found a higher friction coefficient ($\mu_m = 0.45$) for AR and COR-TEN steel [29–31], and a lower value for Zn-coated steel [29,32]. In an internal report, Koike et al. reported similar coefficients for AR and Zn-coated steel [33], with similar values also indicated in Ref. [34], while higher slip factors are found in Ref. [35] for a G350 steel grade with different surface finishings. Again, in Refs. [36,37] much higher slip factors are found on zinc-based metallized faying surfaces connected by a single bolt, but with higher Zn coating thicknesses, 150 μm and 300 μm, and different testing procedure.

The number of test is higher than the minimum required considering the standard deviation s_{Fs}, $n_{\min} > (s_{Fs}/3.5)^2$. Characteristic values of slip factors elaborated by statistical analysis from the experimental mean slip factor and its standard deviation as requested by the standard [22], are summarized in Table 2. For the calculation it has been adopted a fractile $p = 0.05$, confidence level 75%, i.e. $\alpha = 0.25$, a number of test n = 16; the tolerance factor $k_{\alpha,n\text{-}1,p}$ is then estimated by the Monti-Petrone expression, as it well approximates the inverse cumulative distribution function for the noncentral *t*-distribution [38,39]:

$$k_{\alpha,n-1,p} \approx k_{MP1,\alpha,n-1,p} = \frac{z_p}{A}\frac{4n-6}{4n-5} + z_\alpha\sqrt{\frac{1}{n-1} + \frac{1}{2(n-1)}\left(\frac{z_p}{A}\right)^2} \tag{9}$$

with

$$A = 1 - \frac{1+z_\alpha^2}{2(n-1)} \tag{10}$$

In relation to the preload obtained at the prescribed torque, displayed in Fig. 6(b), dispersion of data is very low, with linear relationships observed for all surface finishes. Results are aligned with outcomes obtained in terms of slip factor. Bolts in Zn-coated joints lead to higher tension than in COR-TEN and AR steel joints, which is reflected by the calculated friction coefficients. Since the bolts are the same for all joints, it appears that the torque required to overcome plate/washer contact friction, term $\mu_c r_c F$ in Eq. (1), diminishes from AR to Zn-coated conditions. Values obtained with Eq. (3) are also plotted in Fig. 6(b) together with the experimental data. This expression is simpler than Eq. (1) as it does not consider the different contributions of the applied torque, leading to a good estimation for Zn-coated plates but overestimated values for the other surface finishes.

3.2. Effect of repeated tightening

It is interesting to note that repeated tightening of bolts is hugely detrimental to their efficiency, especially at higher loads, as has been demonstrated in other studies in the literature [2]. Even after 3/4 tightening, the load cell reported 30–40% loss of preload and very low slip resistance of the joint. This is certainly due to plastic deformation of the threads, with no further possible pre-tensioning.

3.3. Design standards

European standard EN 1993 1-1, or EC3 [15], states that bolts should be preloaded to $F_{p,C} = 0.7 f_{ub} A_s$ in the case of bolted shear connections for Category C – Slip-resistant at ultimate limit state. Slip should not occur at the ultimate limit state; therefore, the designed ultimate shear load should not exceed the design slip resistance given by:

Table 2
Statistical elaboration of data.

Surface treatment	$n_{\min}$	n	p	α	z_p	z_α	μ_m	s_μ	$k_{\alpha,n\text{-}1,p}$ [38]	μ
AR	9.4	16	0.05	0.75	1.6449	0.6745	0.242	0.026	1.974	0.191
COR-TEN	5.7						0.372	0.031		0.311
Zn-coated	8.3						0.298	0.030		0.239

$$F_{s,Rd} = \frac{k_s n \mu}{\gamma_{M3}} F_{p,C} \quad (11)$$

where $k_s = 1$ for normal holes, n is the number of friction planes, $\gamma_{M3} = 1.25$ for ultimate state design, and μ is the slip factor obtained by either specific tests for the friction surface in question or, where relevant, by referencing Table 3 for surface finish grades A to D. A comparison between the requirements of EC3 and the experimental slip strength obtained during testing with the M16 8.8 bolt is shown in Fig. 8 for classes ranging from $k = 0.1$ to $k = 0.2$, $A_s = 157$ mm^2, $f_{ub} = 800$ MPa, and $F_{p,C} = 87.92$ kN.

Despite the bolt k-class, the strength of the tested joints was in line with surface grades C (COR-TEN) and D, or even lower, at the highest k-class. This outcome suggests that experimental characterisation of non-standard surface finishes is necessary where safety requirements are paramount.

3.4. FEA and surface topography

An estimation of the contact pressure distribution and sliding region, shown Fig. 9, was obtained via FEA. The estimated contact pressure, as a function of distance from the hole edge in the longitudinal and transversal directions with respect to the load axis, exhibits a relatively uniform distribution with higher values near the edge. Highest values are obtained after preloading (slip 0 condition), while the pressure does not change along the transversal direction during the slip process, but diminishes along the longitudinal direction, see Fig. 9(a). Finally, reproduction of the force-slip curves of the first test set is shown in Fig. 9 (b) using the friction model parameters specified in Table 4. Despite oscillations in the experimental curves, matching indicates that the model correctly describes the phenomenon.

Fig. 10 displays the acquired surface topography and roughness along the sliding path starting from the hole edge. It can be observed that the AR roughness did not change significantly during sliding, which is in alignment with data from the literature for this type of surface [34, 39,40]. The same holds true to a large extent for COR-TEN steel, while the Zn coating was abruptly abraded during sliding in regions of maximum contact pressure, as though an increasing amount of material was accumulated and dragged along.

4. Conclusions

In the present study, S235J steel bolted joints with as-rolled, COR-TEN and Zn-coated finishes were tested to determine the effective slip strength. The surface roughness of each sample was examined with an optical profilometer, and the contact pressure estimated with an FEA model. The following conclusions can be drawn.

1 correspondence between measures and theoretical models for the torque-preload relationship was confirmed;
2. regardless of the surface finish, the slip factor decreases by 10–15% as the tightening torque increases;
3. the characteristic slip factors, calculated by the required statistical approach, are 0.311, 0.239 and 0.191 for COR-TEN, Zn-coated and AR conditions, respectively;

Table 3
Classification of friction surfaces according to EN 1090–2:2018 [22].

Surface treatment	Grade	Slip coefficient μ
Pickling surfaces with steel shot or sandblast, without oxidation or corrosion	A	0.5
Pickling surfaces with steel shot or sandblast and coated	B	0.4
Clean surfaces with brushed steel or flame-free, no oxides	C	0.3
Surfaces such as rolled	D	0.2

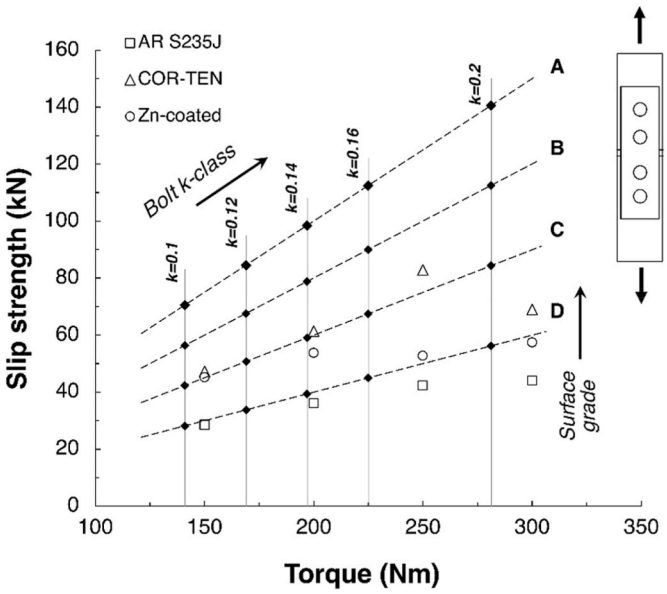

Fig. 8. Experimental slip strength vs EC3.

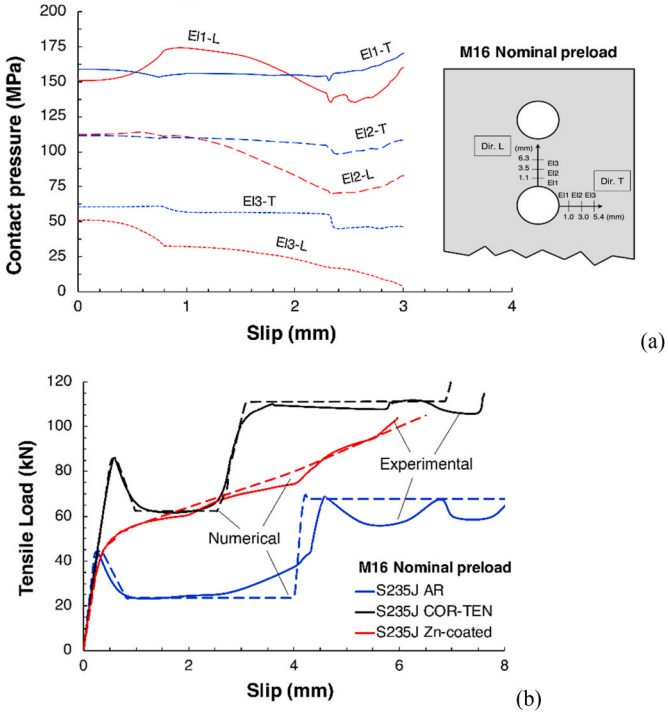

Fig. 9. FEA modelling (a) contact pressure; (b) slip dynamics reproduction.

Table 4
Matching FE parameters at nominal preload.

Surface	μ_s	μ_k	d_c	v_s (m/s)
As rolled	0.21	0.09	$6.5{\cdot}10^{3}$	–
COR-TEN	0.31	0.16	$5.1{\cdot}10^{3}$	–
Zn-coated	0.34	0.22	–	$4.0{\cdot}10^{-4}$

4. despite the bolt k-class, the strength of the tested joints was in line with surface grades C (COR-TEN) and D; however, EC3 can assign relevant surface classes that overestimate the joint strength, for which experimental determination of the slip factor is required

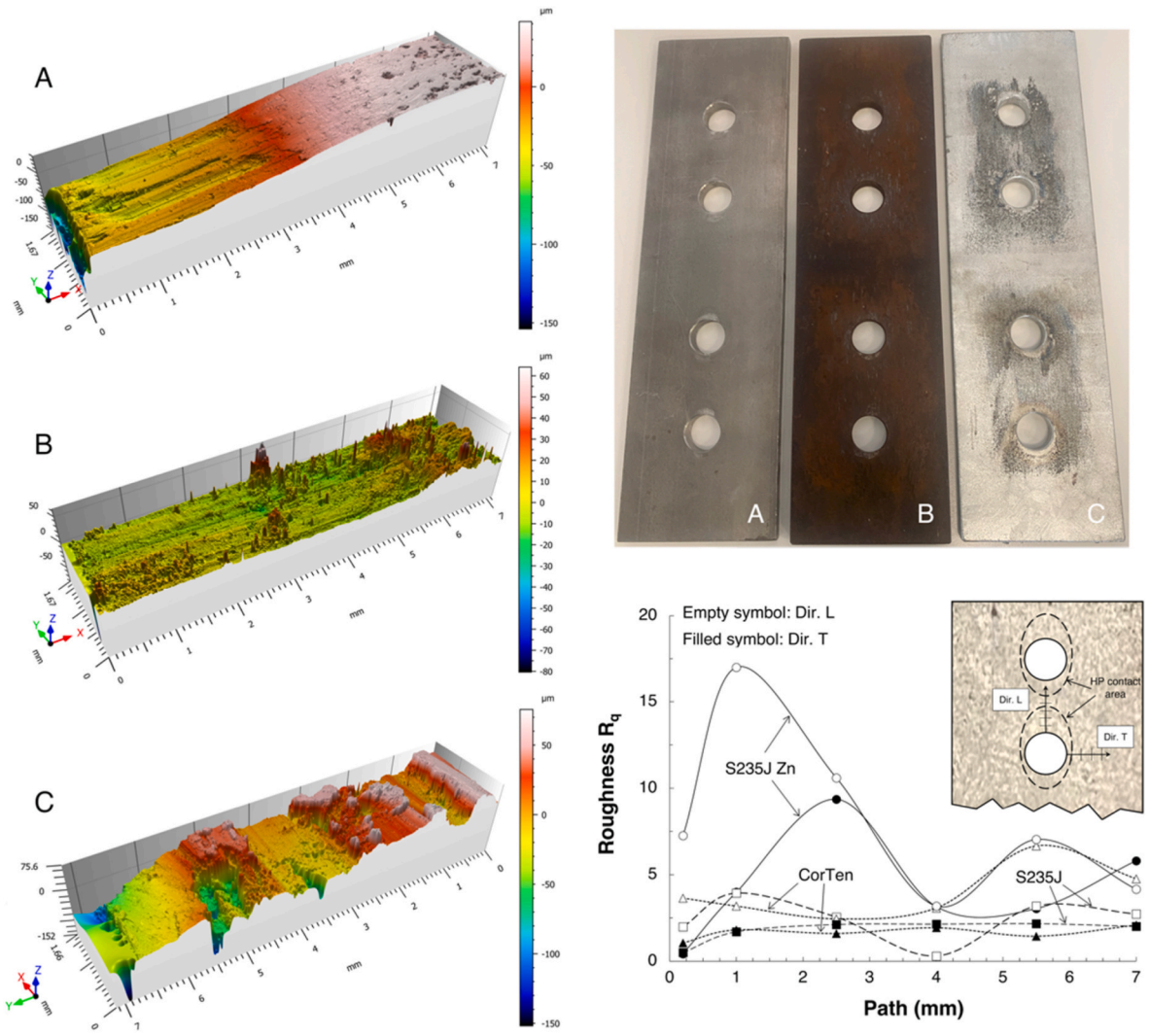

Fig. 10. Optical profilometer topography and roughness measurements.

5. topography measurements of sliding surfaces highlight the fact that friction is a local mechanism, that can be extremely variable;
6. the relation of slip coefficient with surface roughness is confirmed;
7. a reliable FEA modelling is possible providing useful hints for a joint design.

CRediT authorship contribution statement

L. Collini: Data curation, Formal analysis, Investigation, Methodology, Software, Writing – original draft, Writing – review & editing. **R. Garziera:** Conceptualization, Formal analysis, Visualization. **A. Corvi:** Data curation, Formal analysis, Software. **G. Cantarelli:** Data curation, Formal analysis, Validation.

Declaration of competing interest

The authors declare that they have no known competing financial interests or personal relationships that could have appeared to influence the work reported in this paper.

Data availability

Data will be made available on request.

Acknowledgment

This research was granted by University of Parma through the action "*Bando di Ateneo 2021* per *la ricerca*" co-funded by MUR-Italian Ministry of Universities and Research - D.M. 737/2021 - PNR - PNRR - NextGenerationEU.

References

[1] H.L. Whittermore, G.W. Nusbaum, E.O. Seaquist, The Relation of Torque to Tension for Thread Locking Devices, vol. 7, Bureau of Standards J Res, 1931, pp. 945–1016.
[2] Y. Jiang, J. Chang, C.-H. Lee, An experimental study of the torque-tension relationship for bolted joints, Int. J. Mater. Prod. Technol. 16 (4/5) (2001) 417–429.
[3] S.A. Nassar, H. El-Khiamy, G.C. Barber, Q. Zou, T.S. Sun, An experimental study of bearing and thread friction in fasteners, ASME J Tribol 127 (2005) 263–272.
[4] S.A. Nassar, T.S. Sun, Surface roughness effect on the torque-tension relationship in threaded fasteners, P I Mech Eng J-J-Eng 221 (2) (2007) 95–103.
[5] J.H. Bickford, An Introduction to the Design and Analysis of Bolted Joints, third ed., Marcel Dekker, New York, 1997.
[6] D. Croccolo, M. De Agostinis, N. Vincenzi, Failure analysis of bolted joints: effect of friction coefficients in torque–preloading relationship, Eng. Fail. Anal. (2011) 18364–18373.
[7] D. Hinse, M. Thode, A. Rademacher, K. Pantke, C. Spura, Numerical identification of position-dependent friction coefficients from measured displacement data in a bolt-nut connection, Results Eng 19 (2023) 101214.
[8] Y. Shi, M. Wang, Y. Wang, Analysis on shear behavior of high-strength bolts connection, Int J Steel Struct 11 (2) (2011) 203–213.

[9] A. Wang, Z. Zhang, J. Ji, Y. Liu, Study on neutral axis location of common bolts of flush end-plate connections, Results Eng 16 (2022) 100683.
[10] R. Budynas, K. Nisbett, Shigley's Mechanical Engineering Design, eleventh ed., McGraw-Hill, New York, 2020.
[11] T. Sakai, Bolted Joint Engineering: Fundamentals and Applications, Beuth Verlag, Berlin, 2008.
[12] Y.-Q. Wang, J.-K. Wu, H.-B. Liu, K. Kuang, X.-W. Cui, L.-S. Han, Analysis of elastic interaction stiffness and its effect on bolt preloading, Int. J. Mech. Sci. 130 (2017) 307–314.
[13] Y.-h. Huang, R.-h. Wang, J.-h. Zou, Q. Gan, Finite element analysis and experimental study on high strength bolted friction grip connections in steel bridges, J Const Steel Res 66 (6) (2010) 803–815.
[14] R.A. Ibrahima, C.L. Pettit, Uncertainties and dynamic problems of bolted joints and other fasteners, J. Sound Vib. 279 (2005) 857–893.
[15] EN 1993 1–8, Eurocode 3. Design of Steel Structures. Part 1–8: Design of Joints, 2003.
[16] EN ISO 891-1, Mechanical Properties of Fasteners Made of Carbon Steel and Alloy Steel — Part 1: Bolts, Screws and Studs with Specified Property Classes — Coarse Thread and Fine Pitch Thread, 2013.
[17] EN 14399-1, High-strength Structural Bolting Assemblies for Preloading – General Requirements, 2015.
[18] Specification for Structural Joints Using ASTM A325 or A490 Bolts, American Institute of Steel Construction, Inc., Chicago, 1980.
[19] Standard Specifications for Highway Bridges, fourteenth ed., American Association of State Highway and Transportation Officials, 1989.
[20] British Standards Institution, Steel, Concrete and Composite Bridges. Part 3 – Code of Practice for Design of Steel Bridges, 1982. BS 5400.
[21] EN 14399-2, High-strength Structural Bolting Assemblies for Preloading – Part 2: Suitability for Preloading, 2015.
[22] EN 1090-2, Execution of Steel Structures and Aluminium Structures – Part 2: Technical Requirements for Steel Structures – Annex G, 2018.
[23] EN 10025-2, Hot Rolled Products of Structural Steels – Part 2: Technical Delivery Conditions for Non-alloy Structural Steels, 2004.
[24] EN 10025-5, Hot Rolled Products of Structural Steels– Part 5: Technical Delivery Conditions for Structural Steels with Improved Atmospheric Corrosion Resistance, 2005.
[25] ISO 1461, Hot Dip Galvanized Coatings on Fabricated Iron and Steel Articles – Specifications and Test Methods, 2022.
[26] J.T. Oden, J.A.C. Martins, Models and computational methods for dynamic friction phenomena, Comp Meth App Mech Eng 52 (1985) 527–634.
[27] D. Hess, A. Soom, Friction at a lubricating line contact operating at oscillating sliding velocities, ASME J Trib 112 (1) (1990) 147–152.
[28] R. Stribeck, Z. Des. Vereines Dtsch. Ingenieure 46 (38–39) (1902).
[29] W. Eccles, I. Sherrington, R.D. Arnell, Frictional changes during repeated tightening of zinc plated threaded fasteners, Tribol. Int. 43 (2010) 700–707.
[30] C. Heistermann, W. Husson, M. Veljkovic, Flange Connection vs. Friction Connection in Towers for Wind Turbines. Proc. Of Nordic Steel and Construction Conference, Malmö, Sweden, 2009.
[31] C. Heistermann, M. Veljkovic M, R. Simões, C. Rebelo, L. Simões da Silva, Design of slip resistant lap joints with long open slotted holes, J Const Steel Res 82 (2013) 223–233.
[32] Y. Koike, K. Terao, An Experimental Study on Slip Strength of HSFG Bolted Joints Treated with High-Friction Inorganic Zinc-Rich Paint. Internal Report, Yokogawa Bridge Corp. Research Laboratory, Japan, 2003.
[33] A. Cruz, R. Simões, R. Alves, Slip factor in slip resistant joints with high strength steel, J Const Steel Res 70 (2012) 280–288.
[34] A. Trindade, Characterization of strength-shift behavior of bolts connected with and without, Preloading J Mech Eng Autom 8 (2018) 9–16.
[35] A.W. Lacey, W. Chen, H. Hao, K. Bi, Experimental and numerical study of the slip factor for G350-steel bolted connections, J Const Steel Res 158 (2019) 576–590.
[36] C.-D. Annan, A. Chiza, Characterization of slip resistance of high strength bolted connections with zinc-based metallized faying surfaces, Eng. Struct. 56 (2013) 2187–2196.
[37] C.-D. Annan, A. Chiza, Slip resistance of metalized-galvanized faying surfaces in steel bridge construction, J Const Steel Res 95 (2014) 211–219.
[38] G. Monti, F. Petrone, Test-based calibration of safety factors for capacity models, J. Struct. Eng. 142 (11) (2016) 1–12.
[39] D. Li, D. Botto, R. Li, C. Xu, W. Zhang, Experimental and theoretical studies on friction contact of bolted joint interfaces, Int. J. Mech. Sci. 236 (2023) 107773.
[40] E. Maiorana, P. Zampieri, C. Pellegrino, Experimental tests on slip factor in friction joints: comparison between European and American Standards, Fract Struct Int 43 (2018) 205–217.